JOURNAL OF VIROLOGY, Feb. 2006, p. 1087–1097 Vol. 80, No. 3
0022-538X/06/$08.00+0 doi:10.1128/JVI.80.3.1087–1097.2006

Bidirectional Virus Secretion and Nonciliated Cell Tropism following Andes Virus Infection of Primary Airway Epithelial Cell Cultures

Regina K. Rowe[1] and Andrew Pekosz[1,2]*

Departments of Molecular Microbiology[1] and Immunology and Pathology,[2] Washington University School of Medicine, St. Louis, Missouri 63110

Received 3 August 2005/Accepted 2 November 2005

Hantavirus pulmonary syndrome (HPS) is an acute disease resulting from infection with any one of a number of New World hantaviruses. HPS has a mortality rate of 40% and, unlike many other severe respiratory diseases, often occurs in young, healthy adults. Infection is usually initiated after inhalation of rodent excreta containing virus particles, but human-to-human transmission has been documented. Postmortem tissue samples show high levels of viral antigen within the respiratory endothelium, but it is not clear how the virus can traverse the respiratory epithelium in order to initiate infection in the microvasculature. We have utilized Andes virus infection of primary, differentiated airway epithelial cells to investigate the ability of the virus to interact with and cross the respiratory epithelium. Andes virus infects the Clara and goblet cell populations but not the ciliated cells, and this infection pattern corresponds to the expression of β_3 integrin, the viral receptor. The virus can infect via the apical or basolateral membrane, and progeny virus particles are secreted bidirectionally. There is no obvious cytopathology associated with infection, and β_3 integrins do not appear to be critical for respiratory epithelial cell monolayer integrity. Our data suggest that hantavirus infection of the respiratory epithelium may play an important role in the early or prodrome phase of disease as well as serving as a source of virus involved in transmission.

Andes virus (ANDV) is a New World hantavirus and a causative agent of hantavirus pulmonary syndrome (HPS) in South America (10, 53). The New World hantaviruses also include viruses such as Sin Nombre virus, which is a major cause of HPS (8, 33) in North America. Outbreaks of HPS result in mortality rates of approximately 40% (44), irrespective of age or immune status. Disease begins with a prodrome consisting of fever, myalgia, and dyspnea, and progresses rapidly to pulmonary microvascular leakage, respiratory distress, and shock (20). Hantaviruses infect distinct rodent hosts asymptomatically and persistently (8, 33), and most HPS cases can be traced to inhalation of virus-containing excreta from persistently infected rodents (33, 53), but there is documented evidence of person-to-person transmission with ANDV (36).

HPS is not characterized by significant cytopathology within the respiratory epithelium or endothelium (68). This pathology contrasts with other respiratory pathogens, such as influenza A virus, which primarily infect epithelial cells, resulting in high levels of cell death and tissue damage (26). In fact, hantavirus pathogenesis is best compared to viruses such as measles virus (32, 50) and Epstein-Barr virus (54) that interact initially but transiently with the respiratory epithelium in order to gain access to other tissues and cell types that are the major sites for viral replication. The initial interactions of hantaviruses within the respiratory tract are poorly understood; however, following inhalation the virus must traverse the respiratory tract to gain access to the pulmonary epithelium and endothelium where disease pathology is localized. Therefore, viral interactions with the respiratory epithelium may play an important role in hantavirus infection and disease.

There is a significant amount of evidence suggesting a role for the respiratory epithelium during hantavirus infection. First, transmission to humans usually occurs via inhalation of aerosolized rodent excreta; therefore, the initial tissues exposed to the virus would be the respiratory epithelium. Second, the ability of ANDV to spread person-to-person suggests alternate means of transmission—most likely exposure to virus-containing aerosols or droplets and/or infected tissues or fluids. One documented ANDV outbreak in Argentina resulted in a cluster of cases, specifically, health care workers (36). Close contact with infected individuals, not exposure to infected rodents, was determined to be the primary risk factor in this cluster of HPS cases (36). Finally, viral pathogenesis and transmission studies in the primary ANDV rodent reservoir, *Oligoryzomys longicaudatus*, demonstrated viral antigen in the lung epithelium and endothelium (35). Transmission between animals was primarily mediated by direct physical interaction between animals (biting, grooming, or exposure to respiratory secretions) and not by exposure to bedding from cages of infected animals (35).

Currently, the only model for HPS disease is infection of Syrian golden hamsters with South American hantaviruses, including ANDV and Maporal virus (18, 31). Intramuscular infection of hamsters results in a disease course similar to that in humans with symptoms beginning 8 to 10 days postinfection and mortality within 24 h after symptom onset (18). Mortality rates can reach 100%, and pathology is localized to the lungs, with the characteristics of HPS including interstitial pneumonia and pulmonary microvascular leakage (18, 31). Virus can be isolated from oropharyngeal throat swabs but is absent from the salivary glands (31), suggesting productive infection of the

* Corresponding author. Mailing address: Department of Molecular Microbiology, Washington University School of Medicine, Campus Box 8230, 660 S. Euclid Ave., St. Louis, MO 63110. Phone: (314) 747-2132. Fax: (314) 362-7325. E-mail: pekosz@borcim.wustl.edu.

upper airways. Determining the role of the respiratory epithelium during hantavirus infection will provide insights into the early stages (prodrome) of hantavirus infection, dissemination to other tissues in the host, and virus transmission. However, animal studies using hantaviruses are complicated by the requirement for high-containment facilities (biosafety level 4), making it difficult to define key steps during in vivo virus replication.

The airway epithelium is a primary defense providing protection from inhaled pathogens, forming a particle-impermeable barrier as well as producing mucus and mucous proteins to trap and expel foreign materials (62). Well-differentiated, primary respiratory epithelial cell culture models have provided insights into the interactions of many respiratory viruses with the respiratory epithelium, including adenovirus (37, 51, 57, 66, 67), human coronavirus 229E (58), human parainfluenza virus (hPIV) (69), influenza (29), and respiratory syncytial virus (RSV) (28, 70). In this study, we utilized primary hamster tracheal epithelial cells (TECs) to study the replication and tropism of ANDV within the respiratory epithelium.

MATERIALS AND METHODS

Reagents and antibodies. The components in TEC basic medium, proliferation medium, and maintenance medium (TEC MM) were prepared as previously described (43). Rabbit anti-hamster Clara cell secretory protein (CCSP; 1:500 for immunofluorescence and 1:2,000 Western blotting) was kindly provided by Gurmukh Singh (VA Medical Center, Pittsburgh, PA). The mouse anti-Sin Nombre virus (SNV) nucleocapsid (N) antibody (1:500 for immunofluorescence, 1:2,000 for Western blotting, and 1:1,000 for immune plaque assay) was courtesy of Stuart Nichol (Centers for Disease Control and Prevention, Atlanta, GA). Anti-ANDV human convalescent-phase sera (1:150 for immunofluorescence) was kindly provided by Stephen St. Jeor (University of Nevada, Reno, NV). Other primary antibodies were purchased as follows: mouse anti-mucin 5AC (MUC5AC, 1:100 for immunofluorescence; NeoMarkers, Freemont, CA), mouse anti-β-tubulin IV (1:100 for immunofluorescence; BioGenex, San Ramon, CA), and rabbit anti-β_3 integrin (1:100 for immunofluorescence; Calbiochem). Secondary antibodies used were as follows: goat anti-mouse conjugated to fluoroscein isothiocyanate (1:250 for immunofluorescence), goat anti-rabbit conjugated to horseradish peroxidase (HRP; 1:7,500 for Western blotting), and goat anti-mouse HRP (1:7,500 for Western blotting and 1:250 for immune plaque assay), all purchased from Jackson ImmunoResearch, Westgrove, PA. For the immunofluorescence assays, the following secondary antibodies (purchased from Molecular Probes, Eugene, OR) were used at 1:500: goat anti-rabbit Alexa Fluor 594, goat anti-human Alexa Fluor 488, goat anti-mouse Alexa Fluor 594, and ToPro3 nuclear stain. HRP-conjugated soybean agglutinin (1:500 for enzyme-linked immunosorbent assay [ELISA]) was purchased from Sigma, St. Louis, MO. Human interleukin-13 (IL-13) was purchased from Biosource (Camarillo, CA).

Hamster and mouse TEC culture. Hamster TEC cultures were isolated and cultured as previously described (43). For goblet cell differentiation, human IL-13 was added to the basolateral medium at a concentration of 10 ng/ml when an air-liquid interface (ALI) was initiated (24) and removed at the time of infection. Mouse TECs from BALB/c (Charles River Laboratories), C57/B6, or $\beta_3^{-/-}$ mice (17) were isolated and cultured similar to hamster TECs according to the methods described by You et al. (64). Transepithelial resistance (TER) was measured as described previously (43).

Immunofluorescence confocal microscopy. At the indicated days postinfection, hamster TECs were processed for indirect immunofluorescence confocal microscopy as described previously (43). Nuclei were then stained with ToPro3 for 15 min at room temperature. Membranes were mounted with Molecular Probes Prolong antifade, and cells were visualized using a Zeiss 510 Meta LSM confocal microscope.

Three-dimensional analysis of confocal microscopy. Z-stacks acquired by indirect immunofluorescence confocal microscopy were analyzed using the Volocity 3D imaging software (Improvision, Lexington, MA) for three-dimensional visualization of confocal imaging.

Tracheal ring sections. Hamster tracheas were isolated as previously described (43), and each trachea was divided into 5 to 6 rings. Rings were washed three times with phosphate-buffered saline (PBS), embedded in OCT tissue embedding medium (Sakura Finetek, Torrance, CA), and flash-frozen in a dry ice-ethanol bath. The embedded rings were sliced into 7-μm sections using a cryostat (Microm, Waldorf, Germany) and mounted on superfrost microscope slides (Fisher Scientific). OCT was removed with PBS washes, and tissue was fixed in 4% paraformaldehyde for 20 min at room temperature. Tissue sections were processed for immunofluorescence confocal microscopy as previously described (43).

ANDV infection. After 10 to 14 days at an ALI, hamster or mouse TECs were infected at the indicated multiplicity of infection (MOI) with ANDV strain 9717869 (courtesy of Stuart Nichol, Centers for Disease Control and Prevention, Atlanta, GA). Mucus was removed by washing the apical chamber twice with warm TEC basic medium. Virus was diluted in TEC MM, and cells were infected via the apical chamber in a total volume of 50 μl for 2 h at 37°C. For infection from the basolateral membrane, virus inoculum was provided in a total volume of 150 μl in the basolateral chamber for 1 h at 37°C, during which the apical surface was left at an ALI. The inoculum was removed, and cells were washed twice with TEC MM, and 50 μl and 0.5 ml of TEC MM was placed in the apical and basolateral chambers, respectively. Apical and basolateral supernatants were collected for further analysis at the time postinfection indicated in the figures and stored at −70°C.

Vero (Vero E6; American Type Culture Collection) cells were cultured in Dulbecco's modified Eagle's medium (DMEM; Sigma, St. Louis, MO) containing 10% fetal bovine serum (FBS; Atlanta Biologicals, Norcross, GA), 2 mM L-glutamine (Invitrogen, Carlsbad, CA), 100 U/ml penicillin, and 100 μg/ml streptomycin (Invitrogen, Carlsbad, CA). Virus was diluted in DMEM with 2% FBS for Vero infections, and cells were exposed to virus for 2 h at 37°C. The cells were washed extensively with PBS, and infected cell supernatants were collected at the indicated times postinfection.

Virus production was measured by either an immune plaque assay or quantitative reverse transcription-PCR (RT-PCR) for the ANDV virus small (S) RNA segment. All infections were performed using institution-approved biosafety level 3 containment procedures.

Immune plaque assay. Apical and basolateral supernatants were serially diluted in DMEM containing 2% FBS. Confluent monolayers of Vero E6 cells in 3.5-cm^2 six-well dishes were infected with the serial dilutions for 1 h at 37°C, with occasional rocking. Inoculum was removed, and cells were overlaid with 1% agarose solution in DMEM containing 2% FBS and penicillin/streptomycin. Infections were incubated at 37°C in 5% CO_2 for 7 days, at which time cells were fixed with 1% formaldehyde solution in PBS. For immunostaining, cells were permeabilized in ice-cold methanol for 5 min and washed two to three times with PBS. Cells were incubated in mouse anti-SNV nucleocapsid antibody for 2 to 3 h at room temperature, with rocking. Cells were washed with PBS and incubated in secondary antibody goat anti-mouse HRP for 2 h at room temperature, with rocking. Cells were washed in PBS, and plaques were visualized by the addition of metal-enhanced diaminobenzidine substrate (Pierce, Rockford, IL).

Quantitative real-time RT-PCR of ANDV S segment. Viral RNA from harvested apical and basolateral supernatants was isolated using the QIAGEN (Valencia, CA) vRNA mini prep kit according to the manufacturer's protocol. S segment RNA copy numbers were determined using the ABI Taqman EZ RT-PCR kit according to the manufacturer's protocol (Applied Biosystems, Foster City, CA). ANDV S segment (GenBank accession number AF291702)-specific primers and a FAM/TAMRA (FAM is 6-carboxyfluorescein; TAMRA is 6-carboxytetramethylrhodamine) probe were designed as follows: forward S segment RNA primer, 5′-GGAAAACATCACAGCACACGAA-3′ (identical to antigenome nucleotides 66 to 87); reverse S segment RNA primer, 5′-CTGCCTTC TCGGCATCCTT-3′ (complementary to antigenome nucleotides 118 to 136); and S segment FAM/TAMRA probe 5′-AACAGCTCGTGACTGCTCG-GCAAAA-3′ (identical to antigenome nucleotides 89 to 113). All were purchased from Applied Biosystems, Foster City, CA. The RT-PCR conditions used were as follows on an ABI 7000 real-time PCR system (Applied Biosystems): (i) reverse transcription at 60°C for 30 min; (ii) denaturation for 2 min at 95°C, and (iii) 40 cycles of PCR amplification, with 30 s of denaturation (at 95°C) and 1 min of annealing and extension (60°C).

A standard curve for S RNA segment copies was generated by transcribing the PciI restriction enzyme-digested vector pGEM ANDV N with the Megascript SP6 kit (Ambion Inc., Austin, TX). The RNA was quantified by measuring the light absorbance at 260 nm. S RNA segment copies were determined compared to an S segment RNA standard curve and then expressed as S segment RNA copies/ml of viral supernatant.

Influenza A virus infection. Differentiated hamster TECs (10 days at ALI) were infected with recombinant influenza A virus A/Udorn/72 as previously described (43). Apical and basolateral media were removed at the indicated

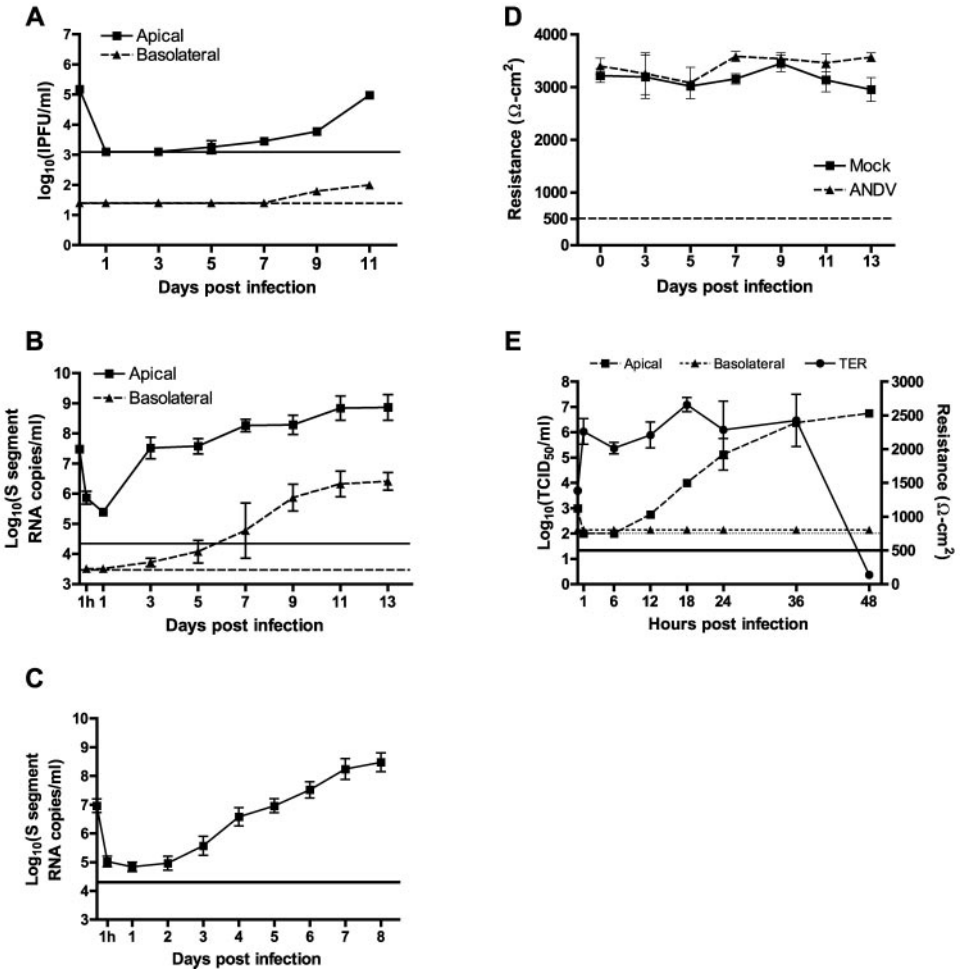

FIG. 1. ANDV replicates in primary hamster TECs without a loss of tight junction integrity. Primary hamster TECs were infected after 10 days at ALI with ANDV, and virus production in both the apical and basolateral supernatants was quantified by either an immune plaque assay (A) or quantitative RT-PCR of the ANDV S segment RNA (B). The horizontal solid and dashed lines indicate the limits of detection for the apical and basolateral samples, respectively. (C) Replication in Vero E6 cells was quantified by RT-PCR. The solid horizontal line indicates the limit of detection. (D) Tight junction integrity during ANDV infection of hamster TECs was monitored by measuring the TER. The dashed line indicates the minimum TER sufficient for tight junction formation and cell polarization. (E) Ten-day differentiated cultures of hamster TECs were infected with influenza A virus (A/Udorn/72) at an MOI of approximately 0.01. Virus production in the apical (squares) and basolateral (triangles) supernatants was monitored by $TCID_{50}$ (left *y* axis). TER (right *y* axis) is shown for infected samples (circles). The dashed and solid lines indicate the limits of detection for the $TCID_{50}$ and TER, respectively.

times postinfection (see Fig. 1E), and transepithelial resistance was measured (43). Infectious virus was quantified by determining the 50% tissue culture infectious dose ($TCID_{50}$) (30).

CCSP secretion, sodium dodecyl sulfate-polyacrylamide gel electrophoresis, and Western blotting. Protein secretion from hamster TECs was monitored at the indicated days postinfection by Western blot analysis. Briefly, 50 μl of mock-infected and virus-infected apical supernatants were diluted in 50 μl of 2× sodium dodecyl sulfate loading buffer solution. For analysis of CCSP, β-mercaptoethanol was added to lysates at a final concentration of 144 mM prior to boiling. Following lysis, samples were boiled for 15 min and run for 3 h at 75 V on either a 15% polyacrylamide gel for separation of ANDV nucleocapsid or a 17.5% polyacrylamide gel containing 4 M urea for separation of CCSP (Bio-Rad, Hercules, CA). Proteins were transferred to polyvinylidene difluoride membrane (Millipore Immobilon-P) at 100 V for 1 h (Mini Transblot, Bio-Rad) and blocked in PBS with 5% dry milk. Blots were incubated in primary and secondary antibodies for 1 h at room temperature, washed with PBS supplemented with 1% Tween 20, and developed using the Amersham ECL-Plus substrate (Amersham, Piscataway, NJ). Protein levels were quantified by phosphorimager analysis (Fujifilm FLA-5000).

Mucin ELISA. At the indicated day postinfection, apical supernatants from mock- and ANDV-infected hamster TECs were lysed by the addition of 10% TX-100 to a final concentration of 1%. Samples were diluted 1:5 in ELISA coating buffer (0.1 M carbonate, 0.1 M bicarbonate, pH 9.5). Fifty microliters of sample was used for coating at 4°C overnight in a 96-well Nunc-Immuno ELISA plate (Nalge Nunc, Rochester, NY). Coating solution was removed, and wells were washed three to four times with PBS and blocked with 50 μl/well 1% bovine serum albumin in PBS with 0.2% Tween 20 (blocking buffer) for 1 h at room temperature. Blocking buffer was removed, and wells were incubated with 50 μl/well HRP-soybean agglutinin (24) for 1 h at room temperature. Wells were washed five times in PBS containing 0.2% Tween 20 and developed with 100 μl of 3,3′,5,5′-tetramethylbenzidine plus ELISA substrate (DakoCytomation, Carpinteria, CA) for 15 min, with shaking at room temperature. The reaction was stopped with 100 μl of 2 M H_2SO_4, and absorbance at 450 nm was measured. The increase (*n*-fold) in hamster TEC supernatants was compared relative to Vero E6 supernatants and expressed as arbitrary units.

RESULTS

ANDV replication in primary hamster TECs. Hamster TECs were infected at an MOI of approximately 0.01, and

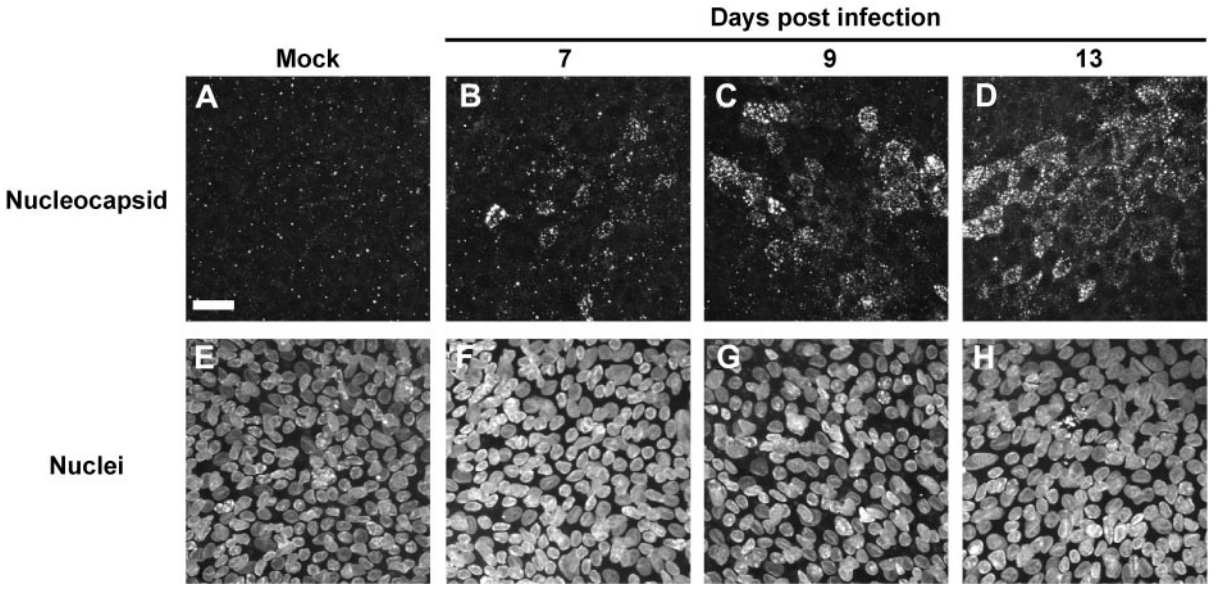

FIG. 2. ANDV replication in hamster TECs results in efficient virus spread. Mock- or ANDV-infected hamster TECs were costained for the virus nucleocapsid protein (A to D) and nuclei (E to H) at various days postinfection and analyzed by indirect immunofluorescence confocal microscopy. Images were acquired with a 63× objective, and the bar represents 25 μm.

virus secretion into the apical and basolateral supernatants was determined at the indicated day postinfection. Infectious virus replication was analyzed by an immune plaque assay (Fig. 1A). Infectious virus particles were detected in the apical supernatant beginning at 5 days postinfection (dpi) and at all subsequent times postinfection. At later times postinfection (9 and 11 dpi) virus was also detected in the basolateral supernatant. The sensitivity of virus detection was significantly improved with the use of a quantitative reverse transcriptase PCR assay based on the ANDV S viral RNA segment. Viral RNA was detected in both the apical and basolateral supernatants (Fig. 1B). When values were adjusted for sample volume, there were approximately 100-fold more virus particles or S RNA copies present in apical samples than in basolateral samples—a value that did not change significantly over the course of the infection. Infection of Vero cells resulted in a comparable amount of virus production (Fig. 1C). The tight junction integrity of the cell culture was unchanged in virus-infected cells as shown by consistent, high TER readings during the entire course of infection (Fig. 1D). This is in contrast to infection with influenza A virus, which resulted in detection of infectious virus particles in the apical but not basolateral supernatant, even at times when the TER readings of the cultures were below 500 $\Omega \cdot cm^2$ (Fig. 1E). The data indicate that ANDV can productively infect hamster TECs, with no loss of monolayer integrity and virus secretion in both the apical and basolateral directions.

After determining the kinetics of virus replication and polarity of virus secretion, we monitored viral antigen spread throughout the culture. The presence of ANDV nucleoprotein was determined by indirect immunofluorescence confocal microscopy of mock- or ANDV-infected hamster TECs at the indicated days postinfection (Fig. 2A to D). Viral antigen was expressed in a small percentage of the cells at 7 dpi, but the percentage of virus-infected cells increased with increasing days postinfection (Fig. 2A to D). Nuclei staining (Fig. 2E to H) showed similar cell numbers with no obvious nuclear fragmentation, blebbing, or chromatin condensation (Fig. 2E to H).

Cell tropism of ANDV infection. The primary hamster TEC culture is composed of a heterogeneous cell population including ciliated, Clara, goblet, and basal cells (43). At the indicated times postinfection, viral antigen (Fig. 3A to E) and specific cellular markers (Fig. 3F to J) were identified by indirect immunofluorescence with specific antibodies, followed by confocal microscopy. Clara cells were identified by expression of CCSP (Fig. 3F and G), a mucus-associated protein constitutively secreted by this cell type (49). Ciliated cells were identified by expression of β-tubulin IV (Fig. 3H and I), a protein localized in the ciliary axonemes of ciliated cells (19). The ciliated and Clara cell populations are the major cellular populations found in the hamster TEC culture (43). Viral antigen was identified in cells expressing CCSP (Fig. 3K and L), while viral antigen was rarely expressed in β-tubulin IV-expressing cells (Fig. 3M and N). These data suggest that the nonciliated cell population, specifically Clara cells, is infected by ANDV. Since goblet cells make up a small percentage (<5%) of the cell population (43), we used IL-13 treatment to enrich this population and upregulate the expression of the goblet cell marker MUC5AC (Fig. 3J) (2, 24, 47). Viral antigen also was found to colocalize with MUC5AC-expressing cells (Fig. 3O). These data indicate that both Clara and goblet cells, but not ciliated cells, are infected by ANDV.

Hantaviruses have been shown to bud into the Golgi apparatus with concomitant transport of virus-containing vesicles to the plasma membrane, leading to release of virus particles (45, 46). In order to better visualize the intracellular location of virus-containing vesicles, we reconstructed three-dimensional images of ANDV-infected hamster TECs from Z-stacks acquired from the immunofluorescence confocal microscopy.

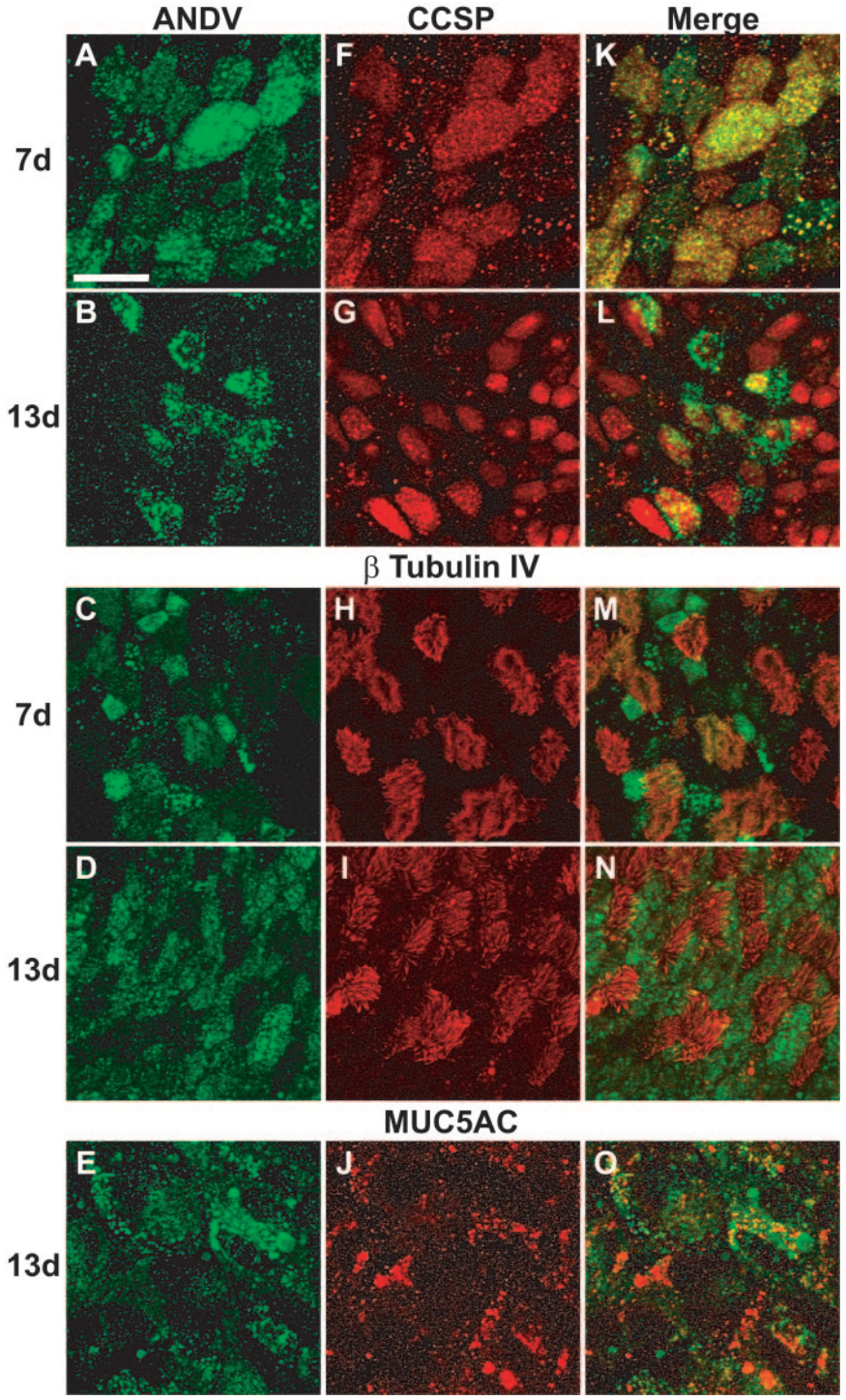

FIG. 3. ANDV infects the nonciliated secretory cell population. ANDV-infected hamster TECs at 7 and 13 dpi were analyzed by indirect immunofluorescence confocal microscopy by costaining for viral antigen (green) (A to E) and cell type-specific markers (red): Clara cells were stained for CCSP (F and G), ciliated cells were identified by β-tubulin IV staining (H and I), and goblet cells were identified by MUC5AC expression (J). Merged images are shown in K to O. Images were acquired with a 63× objective, and the bar represents 25 μm.

Figure 4A and B show a representative three-dimensional reconstruction of hamster TECs stained for viral antigen (green), CCSP (red), and nuclei (blue). The image was rotated with respect to the *x* axis in the *y* direction and shown at either −45° or +90° rotation (Fig. 4A and B, respectively). The corresponding CCSP-positive cells expressing viral antigen in both panels are identified with asterisks for orientation. Intracellular vesicles containing CCSP were found in the apical portion of the cell. However, vesicles containing viral antigen could be identified in both the apical and basolateral (white arrows)

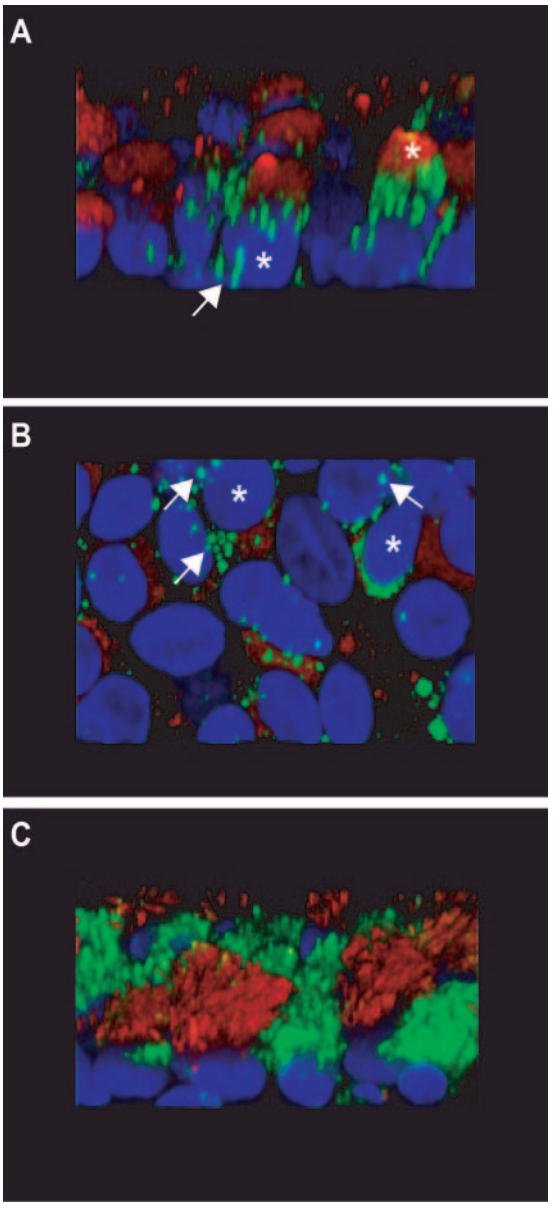

FIG. 4. ANDV infection of hamster TECs results in viral antigen localized to the apical and basolateral regions of the cell. Three-dimensional imaging analysis was performed on Z-stacks acquired by indirect immunofluorescence confocal microscopy. Hamster TECs were costained for the Clara cell marker, CCSP (red), viral antigen (green), and nuclei (blue). Images were then rotated with respect to the *x* axis in the *y* direction. Representative images for rotations of −45° (A) and +90° (B) are shown. The asterisks identify corresponding cells in both panels, while white arrows identify basolaterally localized viral antigen. (C) ANDV-infected hamster TECs immunostained for β-tubulin IV (red), ANDV antigen (green), and nuclei (blue). Image shown at a rotation of −45° with respect to the *x* axis along the *y* axis.

regions, further supporting the data from Fig. 1 indicating bidirectional secretion of ANDV from infected hamster TECs. The lack of ANDV antigen in ciliated cells was also confirmed using three-dimensional image reconstruction (Fig. 4C).

Secretory cell function during ANDV infection. We then determined the effects of infection on the secretory functions

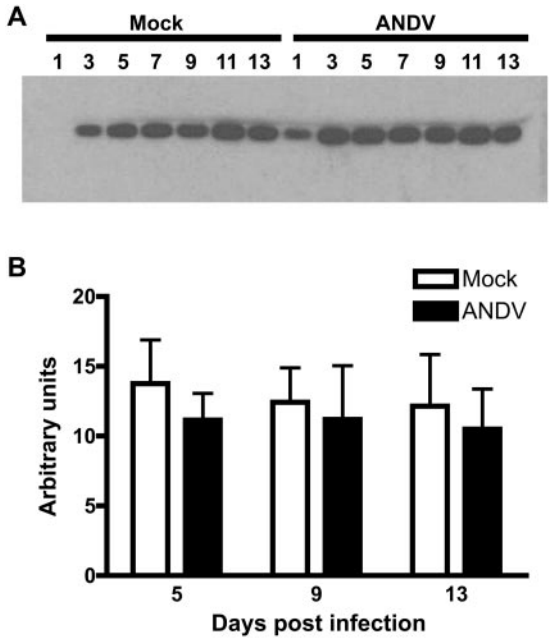

FIG. 5. ANDV infection of hamster TECs does not alter secretory cell function. Secretory cell function during ANDV infection of hamster TECs was monitored by quantifying secretion of CCSP by Western blot analysis (A) and mucus secretion by a mucin ELISA (B).

of Clara and goblet cells. We first measured steady-state secretion of CCSP by Western blotting of apical supernatants (Fig. 5A). Phosphorimager analysis comparing CCSP secretion in mock- and ANDV-infected hamster TECs indicated that at late times postinfection (11 and 13 days) there was less than a 10% change in steady-state CCSP secretion between mock-infected and virus-infected cells (Fig. 5A). Mucin secretion into the apical supernatants was then quantified by performing a mucin ELISA on mock- and ANDV-infected apical supernatants at late time points postinfection (Fig. 5B). There was no significant difference in the steady-state levels of mucin in mock-infected or virus-infected hamster TECs. ANDV infection was confirmed at days 11 and 13 postinfection, with greater than 10^8 S RNA copies detected in the apical supernatants and viral antigen present in a majority of the nonciliated cells (data not shown). The data in Fig. 5 indicate that ANDV infection of nonciliated cells does not alter the steady-state levels of CCSP or mucin in the apical supernatant.

Basolateral infection of hamster TECs. Several viruses display a preference for infecting polarized epithelial cells from either the apical (influenza A [40–42], RSV [70], and hPIV-3 [4, 69]) or the basolateral (vesicular stomatitis virus [23] and adenovirus [57]) membranes. In order to determine whether ANDV could infect hamster TECs from the basolateral membrane, ANDV was exposed to the basolateral membrane of hamster TECs, and virus secretion from the apical and basolateral membranes was monitored by quantitative reverse transcriptase PCR for the S RNA segment (Fig. 6A). Infection kinetics similar to those observed after infection via the apical membrane were observed, with virus release occurring through both the apical and basolateral membranes. TER remained above 1,000 $\Omega \cdot cm^2$ throughout the infection (Fig. 6B), con-

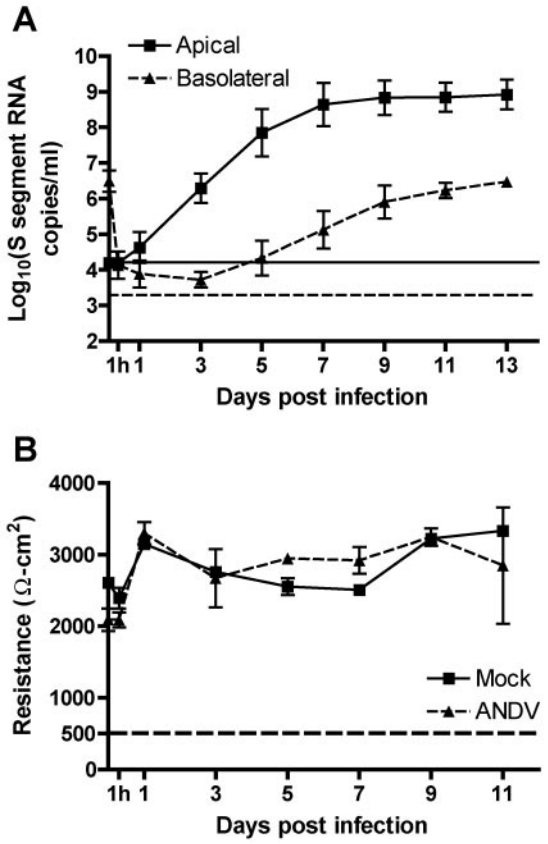

FIG. 6. Hamster TECs are susceptible to ANDV infection via the basolateral membrane. (A) Hamster TECs were infected basolaterally with ANDV, and virus release into the apical and basolateral supernatants was monitored by quantitative RT-PCR of the virus S segment. The horizontal solid and dashed lines indicate the limits of detection for the apical and basolateral samples, respectively. (B) Tight junction integrity during infection was monitored by measuring the TER. The dashed line indicates the minimum TER sufficient for tight junction formation.

firming that there were no breaches in monolayer integrity that might allow virus to diffuse into the apical chamber before initiation of the infection. These results indicate that ANDV is capable of infecting the hamster TECs via the apical or basolateral surfaces.

β_3 integrin expression on hamster TECs. β_3 Integrin has been shown to serve as a receptor for pathogenic hantaviruses (11, 13, 27); therefore, we examined the cell type-specific expression of β_3 integrin in the hamster TECs by indirect immunofluorescence confocal microscopy. Differentiated hamster TECs (20 days at ALI) were costained for β_3 integrin (Fig. 7A and B) and either the ciliated cell marker, β-tubulin IV (Fig. 7D), or the secretory cell marker, MUC5AC (Fig. 7E). The merged images (Fig. 7G and H) indicated that β_3 integrin was expressed on the nonciliated, secretory cell population of the hamster TEC cultures. Hamster tracheal tissue was costained for β_3 integrin (Fig. 7C) and β-tubulin IV (Fig. 7F) and revealed a similar expression pattern with β_3 integrin expressed on the nonciliated cell population (Fig. 7I). These results indicate that β_3 integrin expression correlates with ANDV susceptibility. Unfortunately, we have been unable to block ANDV infection with β_3 integrin-specific reagents (data not shown); therefore, we cannot state unequivocally that β_3 integrin is a functional receptor for ANDV in hamster TEC cultures.

ANDV infection of mouse TECs. Murine β_3 integrin does not serve as a receptor for pathogenic hantaviruses (39); therefore, we were interested in determining whether ANDV could infect mouse TEC cultures. Mouse TECs were infected via the apical membrane, and virus production was monitored. Infection of the mouse TECs was observed as determined by viral RNA and nucleocapsid protein release into the apical supernatant (Fig. 8A); however, infectious virus was below our detection limits. Since disruption of integrin function has been proposed to be a mechanism behind capillary leakage found in HPS pathology (39), we measured the TER of the ANDV-infected cultures and found no loss in tight-junction integrity (Fig. 8B). In order to determine if β_3 integrin expression was important in maintaining airway epithelial culture polarity and tight junction formation, mouse TEC cultures were derived from β_3 integrin-deficient mice (17). TEC cultures from control (C57BL/6) or β_3 integrin knockout mice had a TER indistinguishable from each other and from cultures derived from BALB/c mice (Fig. 7C), indicating that β_3 integrin is not essential to tight junction formation in murine airway epithelial cultures. These data, along with the data shown in Fig. 1, indicate that ANDV disregulation of β_3 integrin function does not result in alteration of monolayer integrity in mouse or hamster airway epithelial cultures.

DISCUSSION

Human infections with hantaviruses are initiated via inhalation of either infected rodent excreta or airborne particles/bodily fluids from HPS patients (36, 44). Following inhalation, the virus must then traverse the respiratory tract to gain access to the respiratory endothelium. Following infection of the respiratory endothelium, the virus can disseminate to other organs and cause disease pathology within the lung. The early steps of hantavirus infection within the respiratory tract have been poorly characterized. Hantaviruses responsible for HPS appear to primarily infect endothelial cells, but the vast majority of studies demonstrating this have focused on pathology in animals showing late stages of disease (18, 31) or on postmortem samples from HPS cases (7, 15, 68). Several studies have demonstrated that in both the rodent host as well as the human host, the viruses that cause HPS can infect the lung epithelium (25, 34–36). In this study, we utilized a primary hamster TEC culture system to characterize hantavirus infection of the respiratory epithelium.

Primary hamster TEC cultures were previously shown to produce a well-differentiated heterogeneous cell population representative of the airway epithelium (43) and therefore provided us with an excellent model to study hantavirus interactions with the respiratory epithelium. ANDV was capable of replicating in the hamster TECs, releasing virus into both the apical and basolateral supernatants. Infection resulted in no obvious cell damage, and basolaterally secreted virus was not due to a breakdown in tight junction integrity as TER remained high throughout infection. This was in contrast to influenza A virus infection, which was shown to cause virus

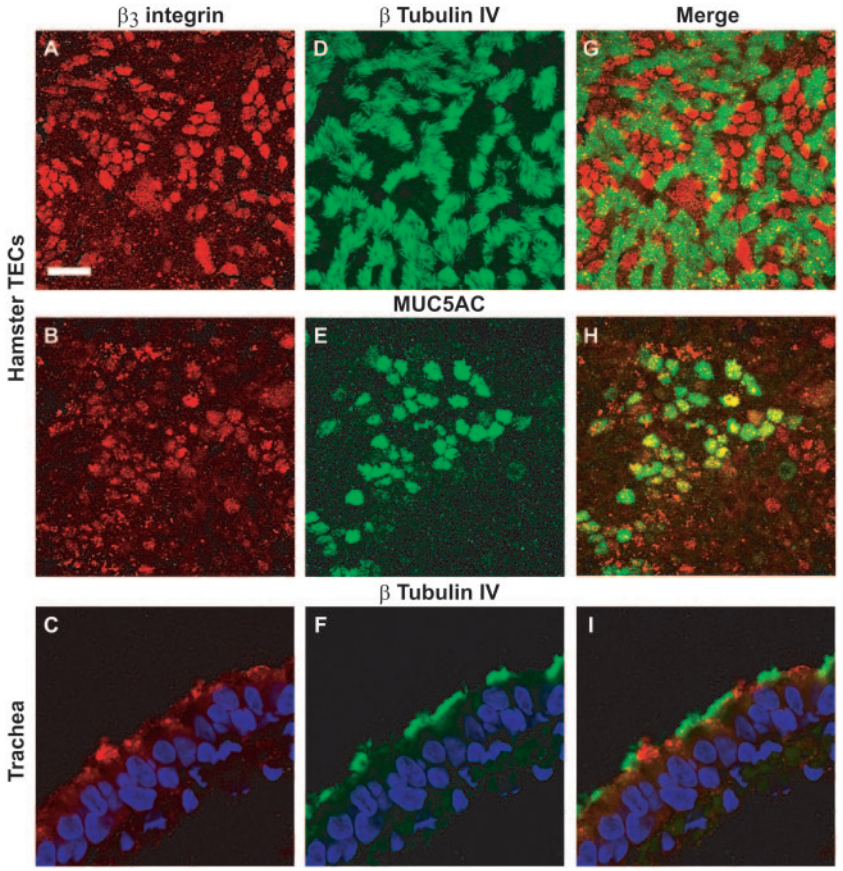

FIG. 7. β3 integrin is expressed on the nonciliated secretory cell population. Differentiated hamster TECs and hamster tracheal tissue were costained by indirect immunofluorescence for β3 integrin (red) (A to C) and cellular markers (green): ciliated cell marker β-tubulin IV (D and F) and secretory cell marker MUC5AC (E). Nuclei of the hamster tracheal epithelium are shown in blue (C, F, and I). Merged images are shown in G to I. Images were acquired with a 63× objective, and the bar represents 25 μm.

particle release exclusively into the apical medium, with a concomitant loss of TER and significant cytopathic effect. Infection of primary, differentiated airway epithelial cells often results in a polarized secretion of the virus; examples include basolateral secretion of adenovirus (57) and apical secretion for RSV (70), hPIV-3 (69), and influenza A virus (Fig. 1). These results suggest that the hantaviruses, specifically ANDV, are released from airway epithelial cells in a bidirectional but not an equivalent manner. Bidirectional virus secretion from polarized cell lines has been demonstrated in Rift Valley fever virus (RVFV)-infected polarized Caco-2 cells, Punto Toro virus-infected polarized Vero cells, and Black Creek Canal virus-infected polarized Vero cells (14, 38). RVFV infection resulted in nearly equivalent amounts of infectious virus particles in both apical and basolateral supernatants, Punto Toro virus yielded higher titers in basolateral supernatants, and Black Creek Canal infection yielded higher titers in apical supernatants. Clearly, this indicates that different bunyaviruses utilize bidirectional secretion to different extents, emphasizing the need to perform these kinds of experiments in relevant cell culture systems.

Our data demonstrate that the respiratory epithelium can serve as a site of hantavirus entry and replication following inhalation. Furthermore, the direct infection of the respiratory epithelium followed by bidirectional virus secretion allows the virus to have direct access to the respiratory endothelium and thus to disseminate and initiate the pathological changes leading to HPS disease. Intramuscular infection in the hamster model of infection or transmission between rodents by biting or scratching results in high levels of virus replication within the lung (5, 6, 16, 18, 31). Infection of hamster TECs via the basolateral membrane, which simulates these routes of infection, also resulted in high levels of virus replication, suggesting that the virus can enter as well as exit via infection of the respiratory epithelium.

Many respiratory viruses infect a specific cell type within the airway epithelium. The paramyxoviruses, RSV (70) and human hPIV-3 (69), target the ciliated cell population; adenovirus infects basal cells (57, 70), while influenza A virus is capable of infecting both ciliated and nonciliated cell populations depending on the virus strain (29). In this study we found that ANDV infection was localized to the nonciliated cell population, specifically colocalizing to Clara and goblet cell populations. Cell tropism was not altered by virus infection via the basolateral membrane (data not shown). Cell type-specific infection by certain viruses can be limited by the expression of the viral receptor. This has specifically been shown for hPIV-3 (69), measles (50, 52), adenovirus (57), and influenza A virus

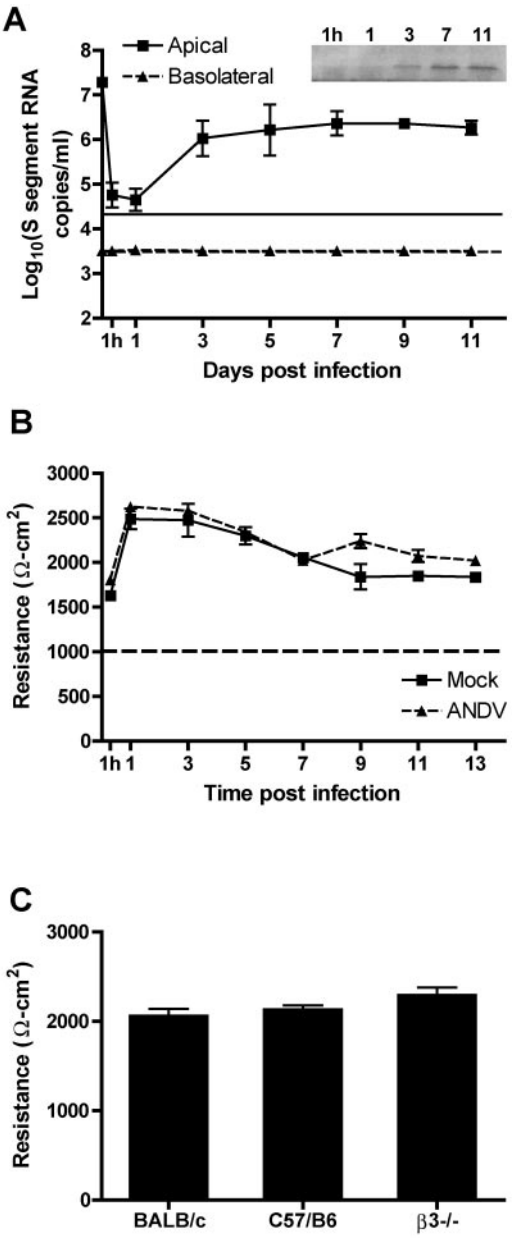

FIG. 8. Mouse TECs are susceptible to ANDV, and β3 integrin is not required for tracheal cell tight junction formation. (A) Mouse TECs were infected apically with ANDV, and virus produced in the apical and basolateral supernatants was measured by quantitative RT-PCR of the virus S RNA segment. Viral nucleocapsid secretion into the apical supernatant was analyzed by Western blotting and shown in the inset of panel A. The horizontal solid and dashed lines indicate the limit of detection for the apical and basolateral samples, respectively. (B) Tight junction integrity during infection was monitored by measuring TER. The dashed line indicates the minimum TER sufficient for tight junction formation and cell polarization. (C) The requirement for β3 integrin in airway epithelial cell tight junction formation was analyzed by monitoring TER in 14-day TEC cultures derived from BALB/c, C57BL/6, or β_3 integrin knockout mice.

(29). β_3 Integrin has been shown to serve as a receptor for pathogenic hantaviruses, including Hantaan virus and SNV (11, 13). Previous studies suggest that β_3 integrin expression can be found on both airway and lung epithelial cells (21, 22, 37, 48). We found that β_3 integrin was expressed in the hamster TEC cultures and was most likely present in both the Clara and goblet cell populations; however, we only colocalized β_3 expression to MUC5AC-positive cells due to antibody limitations. A similar expression pattern for β_3 integrin was found in the hamster trachea. Interestingly, localization of β_3 integrin was primarily on the apical membrane. We cannot rule out the possibility that low levels of β_3 integrin are expressed on the basolateral membrane; however, it is also possible that hantaviruses utilize an alternative receptor that is expressed on the basolateral membrane of epithelial cells.

Infection of laboratory rodents closely mimics infection of the reservoir rodent host, with the murine host having little to no pathology within the lung (1, 9, 63). Replication of ANDV in mouse TECs showed significantly less viral RNA secretion, 10^2-fold to 10^3-fold less, than replication in the hamster TECs and undetectable levels of basolateral viral RNA secretion, suggesting a lack of bidirectional secretion in these cells. Current data suggest that murine β_3 integrin is not capable of mediating hantavirus entry (39). However, there are several studies that indicate that laboratory mice are capable of supporting hantavirus replication in multiple organs including the lung (25, 61, 63), and intraperitoneal infection of mice with Hantaan virus results in mortality (61, 63). Our data, along with that of others, suggest that hantaviruses can replicate in the mouse; therefore, it is likely that virus receptors other than β_3 integrin exist.

Previous data suggests that virus-mediated disregulation of β_3 integrin in endothelial cells may contribute to the pathogenesis seen in HPS (12, 39). β_3 integrin-deficient mice suffer from bleeding disorders (17) and pneumonia (60). By utilizing β_3 integrin-deficient mice, we were able to address the role of this molecule in airway epithelial tight junction integrity. TER of both wild-type and β_3-deficient mouse TECs showed that the expression of β_3 integrin was not required for tight junction integrity of the airway epithelium. These results, together with our data on ANDV infection of hamster TECs, suggest that β_3 integrin plays a much greater role in integrity of the endothelium than the respiratory epithelium.

Many viral infections of the respiratory tract can result in altered secretory cell function, i.e., mucus hypersecretion or goblet cell hyperplasia (28, 55, 56, 59, 65); however, whether these changes result from direct or indirect effects of virus infection remains to be determined. By monitoring secretion of both the CCSP protein and mucins, we determined that hantavirus infection does not alter the steady-state levels of either protein. These data suggest that the secretory cell population is the primary cell type targeted by ANDV in the hamster TEC system, with virus replication not obviously affecting the basic secretory functions of these cell types.

The hamster TECs are a polarized cell culture resulting in cells with distinct apical and basolateral membranes that differ in molecular makeup and function. Many viruses preferentially enter polarized cells via either the apical (influenza, RSV, and hPIV3) or basolateral (vesicular stomatitis virus and adenovirus) membrane. Previous data suggest that for the North American hantavirus, Black Creek canal, entry into polarized Vero cells could only be mediated at the apical membrane (38). Bidirectional infection may be an aspect unique to ANDV or the cell type infected as these results differ from

those seen in the Black Creek Canal studies. However, infection of Caco-2 cells with RVFV could be mediated from both the apical and basolateral membranes (14). The finding that ANDV has the capability to utilize both membrane surfaces of polarized airway epithelial cells leads to many hypotheses on the role of this tissue during ANDV pathogenesis. Infection of the airway epithelium can promote person-to-person transmission with the release of apical virus and also provide the basolaterally released virus easy access to the endothelium, thereby leading to viremia. Infection at both membranes can also provide information on viral entry and receptor usage. Interestingly, infection of primary airway cells with measles virus is mediated preferentially at basolateral membranes, while infection of polarized Vero cells can only occur at the apical plasma membrane (3, 50). This suggests that the bidirectional infection of ANDV in the hamster TEC model may be due to the cell type system used and further supports the use of the primary respiratory cell models as a relevant comparison to infection in vivo.

ACKNOWLEDGMENTS

β_3-deficient mice and wild-type littermates were courtesy of Katherine Weilbaecher and Steven Teitelbaum (Washington University, St. Louis, MO). The authors acknowledge the Washington University Molecular Microbiology Imaging Facility for technical support and all the members of the Pekosz lab for insightful discussions and comments.

This work was supported by the Washington University Lucille P. Markey Pathway in Human Pathobiology predoctoral fellowship (R.K.R.) and Department of Health and Human Services Public Health Services grant R21 AI53381 (A.P.).

REFERENCES

1. **Araki, K., K. Yoshimatsu, B.-H. Lee, H. Kariwa, I. Takashima, and J. Arikawa.** 2004. A new model of Hantaan virus persistence in mice: the balance between HTNV infection and CD8+ T-cell responses. Virology **322:**318–327.
2. **Atherton, H. C., G. Jones, and H. Danahay.** 2003. IL-13-induced changes in the goblet cell density of human bronchial epithelial cell cultures: MAP kinase and phosphatidylinositol 3-kinase regulation. Am. J. Physiol. Lung Cell Mol. Physiol. **285:**L730–739.
3. **Blau, D. M., and R. W. Compans.** 1995. Entry and release of measles virus are polarized in epithelial cells. Virology **210:**91–99.
4. **Bose, S., A. Malur, and A. K. Banerjee.** 2001. Polarity of human parainfluenza virus type 3 infection in polarized human lung epithelial A549 cells: role of microfilament and microtubule. J. Virol. **75:**1984–1989.
5. **Botten, J., K. Mirowsky, D. Kusewitt, M. Bharadwaj, J. Yee, R. Ricci, R. M. Feddersen, and B. Hjelle.** 2000. Experimental infection model for Sin Nombre hantavirus in the deer mouse (*Peromyscus maniculatus*). Proc. Natl. Acad. Sci. USA **97:**10578–10583.
6. **Botten, J., K. Mirowsky, C. Ye, K. Gottlieb, M. Saavedra, L. Ponce, and B. Hjelle.** 2002. Shedding and intracage transmission of Sin Nombre hantavirus in the deer mouse (*Peromyscus maniculatus*) model. J. Virol. **76:**7587–7594.
7. **Colby, T. V., S. R. Zaki, R. M. Feddersen, and K. B. Nolte.** 2000. Hantavirus pulmonary syndrome is distinguishable from acute interstitial pneumonia. Arch. Pathol. Lab. Med. **124:**1463–1466.
8. **Elliott, L. H., T. G. Ksiazek, P. E. Rollin, C. Spiropoulou, S. Morzunov, M. Monroe, C. Goldsmith, C. Humphrey, S. R. Zaki, J. W. Krebs, G. Maupin, K. Gage, J. E. Childs, S. T. Nichol, and C. J. Peters.** 1994. Isolation of the causative agent of hantavirus pulmonary syndrome. Am. J. Trop. Med. Hyg. **51:**102–108.
9. **Fulhorst, C. F., M. L. Milazzo, G. Duno, and R. A. Salas.** 2002. Experimental infection of the Sigmodon alstoni cotton rat with Cano Delgadito virus, a South American hantavirus. Am. J. Trop. Med. Hyg. **67:**107–111.
10. **Galeno, H., J. Mora, E. Villagra, J. Fernandez, J. Hernandez, G. J. Mertz, and E. Ramirez.** 2002. First human isolate of hantavirus (Andes virus) in the Americas. Emerg. Infect. Dis. **8:**657–661.
11. **Gavrilovskaya, I. N., E. J. Brown, M. H. Ginsberg, and E. R. Mackow.** 1999. Cellular entry of hantaviruses which cause hemorrhagic fever with renal syndrome is mediated by β_3 integrins. J. Virol. **73:**3951–3959.
12. **Gavrilovskaya, I. N., T. Peresleni, E. Geimonen, and E. R. Mackow.** 2002. Pathogenic hantaviruses selectively inhibit beta(3) integrin directed endothelial cell migration. Arch. Virol. **147:**1913–1931.
13. **Gavrilovskaya, I. N., M. Shepley, R. Shaw, M. H. Ginsberg, and E. R. Mackow.** 1998. β_3 Integrins mediate the cellular entry of hantaviruses that cause respiratory failure. Proc. Natl. Acad. Sci. USA **95:**7074–7079.
14. **Gerrard, S. R., P. E. Rollin, and S. T. Nichol.** 2002. Bidirectional infection and release of Rift Valley fever virus in polarized epithelial cells. Virology **301:**226–235.
15. **Green, W., R. Feddersen, O. Yousef, M. Behr, K. Smith, J. Nestler, S. Jenison, T. Yamada, and B. Hjelle.** 1998. Tissue distribution of hantavirus antigen in naturally infected humans and deer mice. J Infect. Dis. **177:**1696–1700.
16. **Hinson, E. R., S. M. Shone, M. C. Zink, G. E. Glass, and S. L. Klein.** 2004. Wounding: the primary mode of Seoul virus transmission among male Norway rats. Am. J. Trop. Med. Hyg. **70:**310–317.
17. **Hodivala-Dilke, K. M., K. P. McHugh, D. A. Tsakiris, H. Rayburn, D. Crowley, M. Ullman-Cullere, F. P. Ross, B. S. Coller, S. Teitelbaum, and R. O. Hynes.** 1999. β3-Integrin-deficient mice are a model for Glanzmann thrombasthenia showing placental defects and reduced survival. J. Clin. Investig. **103:**229–238.
18. **Hooper, J. W., T. Larsen, D. M. Custer, and C. S. Schmaljohn.** 2001. A lethal disease model for hantavirus pulmonary syndrome. Virology **289:**6–14.
19. **Jensen-Smith, H. C., R. F. Luduena, and R. Hallworth.** 2003. Requirement for the betaI and betaIV tubulin isotypes in mammalian cilia. Cell Motil. Cytoskeleton **55:**213–220.
20. **Khan, A. S., T. G. Ksiazek, and C. J. Peters.** 1996. Hantavirus pulmonary syndrome. Lancet **347:**739–741.
21. **Kim, H. J., C. A. Henke, S. K. Savik, and D. H. Ingbar.** 1997. Integrin mediation of alveolar epithelial cell migration on fibronectin and type I collagen. Am. J. Physiol. Lung Cell Mol. Physiol. **273:**L134–L141.
22. **Kim, H. J., D. H. Ingbar, and C. A. Henke.** 1996. Integrin mediation of type II cell adherence to provisional matrix proteins. Am. J. Physiol. **271:**L277–L286.
23. **Kobinger, G. P., D. J. Weiner, Q. C. Yu, and J. M. Wilson.** 2001. Filovirus-pseudotyped lentiviral vector can efficiently and stably transduce airway epithelia in vivo. Nat. Biotechnol. **19:**225–230.
24. **Kondo, M., J. Tamaoki, K. Takeyama, J. Nakata, and A. Nagai.** 2002. Interleukin-13 induces goblet cell differentiation in primary cell culture from guinea pig tracheal epithelium. Am. J. Respir. Cell Mol. Biol. **27:**536–541.
25. **Kurata, T., T. F. Tsai, S. P. Bauer, and J. B. McCormick.** 1983. Immunofluorescence studies of disseminated Hantaan virus infection of suckling mice. Infect. Immun. **41:**391–398.
26. **Lamb, R. A., and R. M. Krug.** 2001. *Orthomyxoviridae*: the viruses and their replication, p. 1487–1532. *In* D. M. Knipe, P. M. Howley, D. E. Griffin, R. A. Lamb, M. A. Martin, B. Roizman, and S. E. Straus (ed.), Fields virology, 4th ed. Lippincott Williams & Wilkins, Philadelphia, Pa.
27. **Larson, R. S., D. C. Brown, C. Ye, and B. Hjelle.** 2005. Peptide antagonists that inhibit Sin Nombre virus and Hantaan virus entry through the β_3-integrin receptor. J. Virol. **79:**7319–7326.
28. **Look, D. C., M. J. Walter, M. R. Williamson, L. Pang, Y. You, J. N. Sreshta, J. E. Johnson, D. S. Zander, and S. L. Brody.** 2001. Effects of paramyxoviral infection on airway epithelial cell Foxj1 expression, ciliogenesis, and mucociliary function. Am. J. Pathol. **159:**2055–2069.
29. **Matrosovich, M. N., T. Y. Matrosovich, T. Gray, N. A. Roberts, and H.-D. Klenk.** 2004. Human and avian influenza viruses target different cell types in cultures of human airway epithelium. Proc. Natl. Acad. Sci. USA **101:**4620–4624.
30. **McCown, M. F., and A. Pekosz.** 2005. The influenza A virus M2 cytoplasmic tail is required for infectious virus production and efficient genome packaging. J. Virol. **79:**3595–3605.
31. **Milazzo, M. L., E. J. Eyzaguirre, C. P. Molina, and C. F. Fulhorst.** 2002. Maporal viral infection in the Syrian golden hamster: a model of hantavirus pulmonary syndrome. J. Infect. Dis. **186:**1390–1395.
32. **Moll, M., J. Pfeuffer, H.-D. Klenk, S. Niewiesk, and A. Maisner.** 2004. Polarized glycoprotein targeting affects the spread of measles virus in vitro and in vivo. J Gen. Virol. **85:**1019–1027.
33. **Nichol, S. T., C. F. Spiropoulou, S. Morzunov, P. E. Rollin, T. G. Ksiazek, H. Feldmann, A. Sanchez, J. Childs, S. Zaki, and C. J. Peters.** 1993. Genetic identification of a hantavirus associated with an outbreak of acute respiratory illness. Science **262:**914–917.
34. **Nuovo, G. J., A. Simsir, R. T. Steigbigel, and M. Kuschner.** 1996. Analysis of fatal pulmonary hantaviral infection in New York by reverse transcriptase in situ polymerase chain reaction. Am. J. Pathol. **148:**685–692.
35. **Padula, P., R. Figueroa, M. Navarrete, E. Pizarro, R. Cadiz, C. Bellomo, C. Jofre, L. Zaror, E. Rodriguez, and R. Murua.** 2004. Transmission study of Andes hantavirus infection in wild sigmodontine rodents. J. Virol. **78:**11972–11979.
36. **Padula, P. J., A. Edelstein, S. D. L. Miguel, N. M. Lopez, C. M. Rossi, and R. D. Rabinovich.** 1998. Hantavirus pulmonary syndrome outbreak in Argentina: molecular evidence for person-to-person transmission of Andes virus. Virology **241:**323–330.
37. **Pickles, R. J., D. McCarty, H. Matsui, P. J. Hart, S. H. Randell, and R. C. Boucher.** 1998. Limited entry of adenovirus vectors into well-differentiated

airway epithelium is responsible for inefficient gene transfer. J. Virol. **72:** 6014–6023.
38. **Ravkov, E., S. Nichol, and R. Compans.** 1997. Polarized entry and release in epithelial cells of Black Creek Canal virus, a New World hantavirus. J. Virol. **71:**1147–1154.
39. **Raymond, T., E. Gorbunova, I. N. Gavrilovskaya, and E. R. Mackow.** 2005. Pathogenic hantaviruses bind plexin-semaphorin-integrin domains present at the apex of inactive, bent $\alpha v\beta_3$ integrin conformers. Proc. Natl. Acad. Sci. USA **102:**1163–1168.
40. **Rodriguez-Boulan, E.** 1978. Asymmetric budding of viruses in epithelial molayers: a model system for study of epithelial polarity. Proc. Natl. Acad. Sci. USA **75:**5071–5075.
41. **Rodriguez-Boulan, E.** 1980. Polarized distribution of viral envelope proteins in the plasma membrane of infected epithelial cells. Cell **20:**45–54.
42. **Roth, M. G., J. P. Fitzpatrick, and R. W. Compans.** 1979. Polarity of influenza and vesicular stomatitis virus maturation in MDCK cells: lack of a requirement for glycosylation of viral glycoproteins. Proc. Natl. Acad. Sci. USA **76:**6430–6434.
43. **Rowe, R. K., S. L. Brody, and A. Pekosz.** 2004. Differentiated cultures of primary hamster tracheal airway epithelial cells. In Vitro Cell Dev. Biol. Anim. **40:**303–311.
44. **Schmaljohn, C., and B. Hjelle.** 1997. Hantaviruses: a global disease problem. Emerg. Infect. Dis. **3:**95–104.
45. **Schmaljohn, C., and J. Hooper.** 2001. *Bunyaviridae*: the viruses and their replication, p. 1581–1602. *In* D. M. Knipe, P. M. Howley, D. E. Griffin, R. A. Lamb, M. A. Martin, B. Roizman, and S. E. Straus (ed.), Fields virology, 4th ed. Lippincott Williams & Wilkins, Philadelphia, Pa.
46. **Schmaljohn, C., and C. B. Jonsson.** 2001. Replication of hantaviruses, p. 15–32. *In* C. Schmaljohn and S. T. Nichol (ed.), Hantaviruses. Springer-Verlag, New York, N.Y.
47. **Shahzeidi, S., P. K. Aujla, T. J. Nickola, Y. Chen, M. Z. Alimam, and M. C. Rose.** 2003. Temporal analysis of goblet cells and mucin gene expression in murine models of allergic asthma. Exp. Lung Res. **29:**549–565.
48. **Singh, B., N. Rawlings, and A. Kaur.** 2001. Expression of integrin $\alpha v\beta_3$ in pig, dog and cattle. Histol. Histopathol. **16:**1037–1046.
49. **Singh, G., and S. L. Katyal.** 1997. Clara cells and Clara cell 10-kD Protein (CC10). Am. J. Respir. Cell Mol. Biol. **17:**141–143.
50. **Sinn, P. L., G. Williams, S. Vongpunsawad, R. Cattaneo, and P. B. McCray, Jr.** 2002. Measles virus preferentially transduces the basolateral surface of well-differentiated human airway epithelia. J. Virol. **76:**2403–2409.
51. **Stonebraker, J. R., D. Wagner, R. W. Lefensty, K. Burns, S. J. Gendler, J. M. Bergelson, R. C. Boucher, W. K. O'Neal, and R. J. Pickles.** 2004. Glycocalyx restricts adenoviral vector access to apical receptors expressed on respiratory epithelium in vitro and in vivo: role for tethered mucins as barriers to lumenal infection. J. Virol. **78:**13755–13768.
52. **Tatsuo, H., N. Ono, K. Tanaka, and Y. Yanagi.** 2000. SLAM (CDw150) is a cellular receptor for measles virus. Nature **406:**893–897.
53. **Toro, J., J. D. Vega, A. S. Khan, J. N. Mills, P. Padula, W. Terry, Z. Yadón, R. Valderrama, B. A. Ellis, Carlos Pavletic, R. Cerda, S. Zaki, S. Wun-Ju, R. Meyer, M. Tapia, C. Mansilla, M. Baro, J. A. Vergara, M. Concha, G. Calderon, D. Enria, C. J. Peters, and T. G. Ksiazek.** 1998. An outbreak of hantavirus pulmonary syndrome, Chile, 1997. Emerg. Infect. Dis. **4:**687–694.
54. **Tugizov, S. M., J. W. Berline, and J. M. Palefsky.** 2003. Epstein-Barr virus infection of polarized tongue and nasopharyngeal epithelial cells. Nat. Med. **9:**307–314.
55. **Walter, M. J., N. Kajiwara, P. Karanja, M. Castro, and M. J. Holtzman.** 2001. Interleukin-12 p40 production by barrier epithelial cells during airway inflammation. J. Exp. Med. **193:**339–352.
56. **Walter, M. J., J. D. Morton, N. Kajiwara, E. Agapov, and M. J. Holtzman.** 2002. Viral induction of a chronic asthma phenotype and genetic segregation from the acute response. J. Clin. Investig. **110:**165–175.
57. **Walters, R. W., P. Freimuth, T. O. Moninger, I. Ganske, J. Zabner, and M. J. Welsh.** 2002. Adenovirus fiber disrupts CAR-mediated intercellular adhesion allowing virus escape. Cell **110:**789–799.
58. **Wang, G., C. Deering, M. Macke, J. Shao, R. Burns, D. M. Blau, K. V. Holmes, B. L. Davidson, S. Perlman, and P. B. McCray, Jr.** 2000. Human coronavirus 229E infects polarized airway epithelia from the apical surface. J. Virol. **74:**9234–9239.
59. **Wang, S.-Z., C. L. Rosenberger, Y.-X. Bao, J. M. Stark, and K. S. Harrod.** 2003. Clara cell secretory protein modulates lung inflammatory and immune responses to respiratory syncytial virus infection. J. Immunol. **171:**1051–1060.
60. **Weng, S., L. Zemany, K. N. Standley, D. V. Novack, M. La Regina, C. Bernal-Mizrachi, T. Coleman, and C. F. Semenkovich.** 2003. β_3 Integrin deficiency promotes atherosclerosis and pulmonary inflammation in high-fat-fed, hyperlipidemic mice. Proc. Natl. Acad. Sci. USA **100:**6730–6735.
61. **Wichmann, D., H. J. Grone, M. Frese, J. Pavlovic, B. Anheier, O. Haller, H.-D. Klenk, and H. Feldmann.** 2002. Hantaan virus infection causes an acute neurological disease that is fatal in adult laboratory mice. J. Virol. **76:**8890–8899.
62. **Wu, R.** 1997. Growth and differentiation of tracheobronchial epithelial cells, p. 211–241. *In* J. A. McDonald (ed.), Lung growth and development, vol. 100. Marcel Dekker, Inc., New York, N.Y.
63. **Yoshimatsu, K., J. Arikawa, S. Ohbora, and C. Itakura.** 1997. Hantavirus infection in SCID mice. J. Vet. Med. Sci. **59:**863–868.
64. **You, Y., E. J. Richer, T. Huang, and S. L. Brody.** 2002. Growth and differentiation of mouse tracheal epithelial cells: selection of a proliferative population. Am. J. Physiol. Lung Cell Mol. Physiol. **283:**L1315–1321.
65. **Yuta, A., W. J. Doyle, E. Gaumond, M. Ali, L. Tamarkin, J. N. Baraniuk, M. Van Deusen, S. Cohen, and D. P. Skoner.** 1998. Rhinovirus infection induces mucus hypersecretion. Am. J. Physiol. Lung Cell Mol. Physiol. **274:**L1017–1023.
66. **Zabner, J., P. Freimuth, A. Puga, A. Fabrega, and M. J. Welsh.** 1997. Lack of high affinity fiber receptor activity explains the resistance of ciliated airway epithelia to adenovirus infection. J. Clin. Investig. **100:**1144–1149.
67. **Zabner, J., B. G. Zeiher, E. Friedman, and M. J. Welsh.** 1996. Adenovirus-mediated gene transfer to ciliated airway epithelia requires prolonged incubation time. J. Virol. **70:**6994–7003.
68. **Zaki, S. R., P. W. Greer, L. M. Coffield, C. S. Goldsmith, K. B. Nolte, K. Foucar, R. M. Feddersen, R. E. Zumwalt, G. L. Miller, A. S. Khan, et al.** 1995. Hantavirus pulmonary syndrome. Pathogenesis of an emerging infectious disease. Am. J. Pathol **146:**552–579.
69. **Zhang, L., A. Bukreyev, C. I. Thompson, B. Watson, M. E. Peeples, P. L. Collins, and R. J. Pickles.** 2005. Infection of ciliated cells by human parainfluenza virus type 3 in an in vitro model of human airway epithelium. J. Virol. **79:**1113–1124.
70. **Zhang, L., M. E. Peeples, R. C. Boucher, P. L. Collins, and R. J. Pickles.** 2002. Respiratory syncytial virus infection of human airway epithelial cells is polarized, specific to ciliated cells, and without obvious cytopathology. J. Virol. **76:**5654–5666.